Effect of short-range order on the electronic structure and optical properties of the CuZn alloys: An augmented space approach

Kartick Tarafder,[1] Atisdipankar Chakrabarti,[1,*] Kamal Krishna Saha,[2] and Abhijit Mookerjee[1]
[1]*S.N. Bose National Center for Basic Sciences, JD Block, Sector III, Salt Lake City, Kolkata 700 098, India*
[2]*Theory Department, Max-Planck-Institut für Mikrostrukturphysik, Weinberg 2, D-06120 Halle (Saale), Germany*
(Received 22 May 2006; revised manuscript received 27 July 2006; published 24 October 2006)

In this work we have combined the generalized augmented space method introduced by one of us with the recursion method of [Haydock and Te, Phys. Rev. B **49**, 10845 (1994)] (GASR), within the framework of the local density functional based linear muffin-tin orbitals basis (TB-LMTO). Using this we have studied the effect of short-range ordering and clustering on the density of states, optical conductivity, and reflectivity of 50-50 CuZn alloys. Our results are in good agreement with alternative techniques. We argue that the TB-LMTO-GASR is a feasible, efficient, and quantitatively accurate computational technique for the study of environmental effects in disordered binary alloys.

DOI: 10.1103/PhysRevB.74.144204 PACS number(s): 71.20.Gj, 71.23.−k, 36.40.Cg

I. INTRODUCTION

Binary alloys involving equal proportions of a noble metal Cu and a divalent metal Zn have a stable low-temperature β phase which sits immediately to the right of the pure face-centered-cubic Cu phase in the alloy phase diagram.[1,2] This phase, called β brass, has a body-centered-cubic structure. At high temperatures the alloy forms a disordered body-centered-cubic structure. At around 730 K it orders into the B2 structure with two atoms per unit cell. The alloy satisfies the Hume-Rotherý rules[3] and has the same ratio of valence electrons to atoms. Jona and Marcus[1] have shown from a density functional theory (DFT) based approach that within the local density approximation (LDA), it is the body-centered-based B2 which is the stable ground state. They also showed that if we include the gradient corrections (GGA) then we obtain a tetragonal ground state lower in energy by 0.1 mRy/atom. This is in contradiction with the latest experimental data. The alloying of face-centered-cubic Cu with an equal amount of Zn leads to a body-centered stable phase. Zn has only one more electron than Cu. This is an interesting phenomenon. CuZn alloys also have anomalously high elastic anisotropy. This makes the theoretical study of CuZn an interesting exercise for a proposed theoretical technique.

One of the earliest first-principles density functional based study of the electronic properties of CuZn was by Bansil and Ehrenreich.[4] The authors had studied the complex bands of α phase of CuZn using the Korringa-Kohn-Rostocker (KKR) method coupled with the coherent potential approximation (CPA) to take care of disorder. They commented on the effects of charge transfer and lattice constants on the electronic structure. They found the electronic distribution of this alloy to be of a split band kind with the centers of the Cu and Zn d bands well separated from each other. Their Zn d bands showed hardly any dispersion and were shown only schematically in their figures. In a later work Rowlands *et al.*[5] generalized the CPA to a nonlocal version (NL-CPA) and studied the effects of short-range ordering in CuZn. Their technique was based on an idea of renormalization in reciprocal space suggested by Jarrell and Krishnamurthy.[6]

The order-disorder transition in CuZn is a classical example of a true second-order transition. Several very early investigations on this alloy have been reviewed by Nix and Shockley[7] and Guttman.[8] These investigations, of course, were rather crude, since sophisticated approaches to deal with disordered alloys had really not been developed at that time. However, it was recognized that a knowledge of the short-range order correlations above the critical temperature should be of considerable interest. Early neutron scattering experiments were carried out on β brass by Walker and Keating.[9] The Warren-Cowley short-range order parameter, defined by $\alpha(R)=1-P_{AB}(R)/x$, where x is the concentration of A and $P_{AB}(R)$ is the probability of finding an A atom at a distance of R from a B atom, was directly obtained from the diffuse scattering cross section

$$\frac{d\sigma}{d\Omega} = x(1-x)(b_A - b_B)^2 \sum_R \alpha(R) f(K) \exp(iKR),$$

where b_A, b_B are the scattering lengths of A and B atoms, and $f(K)=\exp(-C|K|^2)$ is the attenuation factor arising from thermal vibrations and static strains. The experimental data for the short-range order parameter as a function of temperature are thus available to us. An Ising-like model using pair interactions was studied by Walker and Chipman[10] and the short-range order was theoretically obtained. However, the pair interactions were simply fitted to the experimental values of the transition temperature T_C and in that sense it was an empirical theory. The experimental estimate of the nearest neighbor Warren-Cowley parameter was found to be varying between −0.171 to −0.182 at around 750 K.

In a later work using the much more sophisticated *locally self-consistent Green function* (LSGF) approach based on the tight-binding linear muffin-tin orbital (TB-LMTO) technique, Abrikosov *et al.*[11] studied CuZn alloys. The authors argued that earlier studies of the mixing enthalpies of CuZn using the standard coherent potential approximation

approaches[12–16] showed significant discrepancies with experiment. The discrepancies were assumed to partly arise from the neglect of charge transfer effects and partly because of short-ranged ordering (SRO). The main thrust of this technique, which was based on an earlier idea of a locally self-consistent multiple scattering (LSMS) by Wang *et al.*,[17] was to go beyond the CPA and include the effects of the immediate environment of an atom in the solid. The LSMS gave an excellent theoretical estimate of the ordering energy in CuZn: 3.37 mRy/atom as compared to the experimental value of 3.5 mRy/atom. The LSGF approach correctly predicted ordering tendency in CuZn on lowering temperature and combining with a cluster variation and Connolly Williams model (CVM-CW) obtained a value of the nearest-neighbor Warren-Cowley SRO parameter $\alpha=-0.15$. Subsequently, Bruno *et al.*[18] proposed a modification of the CPA including the local field effects and showed that charge transfer effects can be taken into account as accurately as the $O(N)$ methods just described. They applied their approach to the CuZn alloys.

One of the earlier works on the optical property of the CuZn alloy was the determination of the temperature variation of optical reflectivity by Muldawer.[19] The author attempted to explain the color of the disordered β-brass CuZn alloy via the internal photoelectric effect.[20] Although the experimental data also contained the contribution from plasma oscillations, the author claimed that the optical reflectivity helps to explain the band picture of the alloys as a function of the interatomic spacing. In order to explain the optical properties, Amar *et al.*[21–23] studied the band structure of CuZn using the KKR method. However, they had used the virtual crystal approximation, replacing the random potential seen by the electrons by an averaged one. This is now known to be particularly inaccurate for split band alloys.

The above discussion was necessary to bring into focus the following points: in the study of alloys such as CuZn it would be interesting to address the effects of charge transfer and short-range ordering. In this paper we shall address exactly these two points. We shall propose the use of the augmented space recursion (ASR) coupled with the tight-binding linear muffin-tin orbitals basis (TB-LMTO)[24] to study the effects of short-range ordering on both the electronic structure and the optical properties of the β-CuZn alloy at 50-50 composition. We should like to stress here that the TB-LMTO-ASR addresses precisely these effects with accuracy: the density functional self-consistent TB-LMTO takes care of the charge transfer, while the local environmental effects which are essential for the description of SRO are dealt with by the ASR. The TB-LMTO-ASR and its advantages have been extensively discussed earlier in a review by Mookerjee,[25] and in a series of articles.[24,26–30] We would like to refer the interested readers to these for details.

II. SPECTRAL FUNCTIONS, COMPLEX BANDS, AND DENSITY OF STATES FOR 50-50 CuZn

In this section we shall introduce the salient features of the ASR which will be required by us in our subsequent discussions.

We shall start from a first principle TB-LMTO set of orbitals[31,32] in the most-localized representation. This is necessary, because the subsequent recursion requires a sparse representation of the Hamiltonian. The TB-LMTO second-order tight-binding Hamiltonian $\mathbf{H}^{(2)}$ is described by a set of *potential parameters*: $\mathbf{C}_R$, $\mathbf{E}_{\nu R}$, $\mathbf{\Delta}_R$, and $\mathbf{o}_R$ which are characteristic of the atoms which sit on the lattice sites labeled by R, and a structure matrix $\mathbf{S}_{RR'}$ which is characteristic of the lattice on which the atoms sit. For a substitutionally disordered alloy, the structure matrix is not random but the potential parameters are and can be described by a set of random *occupation variables* $\{n_R\}$. We may write

$$C_{RL} = C_L^A n_R + C_L^B (1 - n_R)$$

and similar expressions for the other potential parameters. The random site-occupation variables $\{n_R\}$ take values 1 and 0 depending upon whether the muffin-tin labeled by R is occupied by A or B type of atom. The atom sitting at $\{R\}$ can either be of type A $(n_R=1)$ with probability x or B $(n_R=0)$ with probability y.

In the absence of short-range order, the augmented space formalism associates with each random variable n_R an operator $\mathbf{M}_R$ whose spectral density is its probability density,

$$p(n_R) = -\frac{1}{\pi}\lim_{\delta\to 0} \mathrm{Im}\langle\uparrow_R|[(n_R + i\delta)\mathbf{I} - \mathbf{M}_R]^{-1}|\uparrow_R\rangle.$$

The operator $\mathbf{M}_R$ acts on the "configuration space" of the variable n_R, $\mathbf{\Phi}_R$ spanned by the configuration states $|\uparrow_R\rangle$ and $|\downarrow_R\rangle$. The augmented space theorem[26] states that a configuration average can be expressed as a matrix element in the "configuration space" of the disordered system,

$$\langle\langle A(\{n_R\})\rangle\rangle = \langle\{\varnothing\}|\tilde{\mathbf{A}}(\{\mathbf{M}_R\})|\{\varnothing\}\rangle \tag{1}$$

where

$$\tilde{\mathbf{A}}(\{\tilde{\mathbf{M}}_R\}) = \int \cdots \int A(\{\lambda_R\}) \prod d\mathbf{P}(\lambda_R).$$

$\mathbf{P}(\lambda_R)$ is the spectral density of the self-adjoint operator $\tilde{\mathbf{M}}_R$, and the configuration state $|\{\varnothing\}\rangle$ is $\Pi_R^{\otimes}|\uparrow_R\rangle$. Applying Eq. (1) to the Green's function we obtain

$$\langle\langle \mathbf{G}(\mathbf{k},z)\rangle\rangle = \langle \mathbf{k}\otimes\{\varnothing\}|(z\tilde{\mathbf{I}} - \tilde{\mathbf{H}}^{(2)})^{-1}|\mathbf{k}\otimes\{\varnothing\}\rangle, \tag{2}$$

where $\mathbf{G}$ and $\mathbf{H}^{(2)}$ are operators which are matrices in angular momentum space, and the augmented $\mathbf{k}$-space basis $|\mathbf{k}, L\otimes\{\varnothing\}\rangle$ has the form

$$(1/\sqrt{N})\sum_R \exp(-i\mathbf{k}\cdot R)|R, L\otimes\{\varnothing\}\rangle.$$

The augmented space Hamiltonian $\tilde{\mathbf{H}}^{(2)}$ is constructed from the TB-LMTO Hamiltonian $\mathbf{H}^{(2)}$ by replacing each random variable n_R by the operators $\tilde{\mathbf{M}}_R$. It is an operator in the augmented space $\Psi = \mathcal{H}\otimes\Pi_R^{\otimes}\mathbf{\Phi}_R$. The ASF maps a disordered Hamiltonian described in a Hilbert space $\mathcal{H}$ onto an ordered Hamiltonian in an enlarged space Ψ, where the space Ψ is constructed as the outer product of the space $\mathcal{H}$

and configuration space Φ of the random variables of the disordered Hamiltonian. The configuration space Φ is of rank 2^N if there are N muffin-tin spheres in the system. Another way of looking at $\tilde{\mathbf{H}}^{(2)}$ is to note that it is the *collection* of all possible Hamiltonians for all possible configurations of the system.

This equation is now exactly in the form in which the recursion method may be applied. At this point we note that the above expression for the averaged $G_{LL}(\mathbf{k},z)$ is *exact*.

The recursion method addresses inversions of infinite matrices of the type associated with the Green's function.[33] Once a sparse representation of an operator in Hilbert space, $\tilde{\mathbf{H}}^{(2)}$, is known in a countable basis, the recursion method obtains an alternative basis in which the operator becomes tridiagonal. This basis and the representations of the operator in it are found recursively through a three-term recurrence relation. The spectral function is then obtained from the continued fraction

$$\langle\langle G_{LL}(\mathbf{k},z)\rangle\rangle = \cfrac{\beta_{1L}^2}{z-\alpha_{1L}(\mathbf{k})-\cfrac{\beta_{2L}^2(\mathbf{k})}{z-\alpha_{2L}(\mathbf{k})-\cfrac{\beta_{3L}^2(\mathbf{k})}{\ddots}}} = \frac{\beta_{1L}^2}{z-E_L(\mathbf{k})-\Sigma_L(\mathbf{k},z)} \tag{3}$$

$$\cfrac{}{z-\alpha_{NL}(\mathbf{k})-\mathbf{\Gamma}_L(\mathbf{k},z)}$$

where $\mathbf{\Gamma}_L(\mathbf{k},z)$ is the asymptotic part of the continued fraction. The approximation involved has to do with the termination of this continued fraction. The coefficients are calculated exactly up to a finite number of steps $\{\alpha_n,\beta_n\}$ for $n<N$ and the asymptotic part of the continued fraction is obtained from the initial set of coefficients using the idea of Beer and Pettifor's terminator.[34] Haydock and co-workers[35] have carried out extensive studies of the errors involved and precise estimates are available in the literature. Haydock[36] has shown that if we carry out recursion exactly up to N steps, the resulting continued fraction maintains the first $2N$ moments of the exact result.

The self-energy $\Sigma_L(\mathbf{k},z)$ arises because of scattering by the random potential fluctuations.

The average spectral function $\langle\langle A_{\mathbf{k}}(E)\rangle\rangle$ is related to the averaged Green's function in reciprocal space as

$$\langle\langle A_{\mathbf{k}}(E)\rangle\rangle = \sum_L \langle\langle A_{\mathbf{k}L}(E)\rangle\rangle,$$

where

$$\langle\langle A_{\mathbf{k}L}(E)\rangle\rangle = -\frac{1}{\pi}\lim_{\delta\to 0+}\{\mathrm{Im}\langle\langle G_{LL}(\mathbf{k},E-i\delta)\rangle\rangle\}.$$

To obtain the complex bands for the alloy we fix a value for $\mathbf{k}$ and solve for

$$z-E_L(\mathbf{k})-\Sigma_L(\mathbf{k},E)=0.$$

The real part of the roots will give the position of the bands, while the imaginary part of roots will be proportional to the disorder-induced broadening. Since the alloy is random, the bands always have finite lifetimes and are fuzzy.

We have used this reciprocal space ASR to obtain the complex bands and spectral functions for the CuZn alloy. This is shown in Figs. 1 and 2. It should be noted that we have carried out a fully LDA self-consistent calculation using the TB-LMTO-ASR developed by us[37] to obtain the potential parameters. It takes care of the charge transfer effects. For the Madelung energy part of the alloy calculation, we have chosen the approach of Ruban and Skriver.[38]

The two panels of Fig. 1 compare the band structures of pure Cu and pure Zn metals in the same bcc lattice as the 50-50 alloy. We note that the *s*-like bands of Cu and Zn stretch from −0.8 Ry, while the *d*-like states of Zn and Cu, whose degeneracies are lifted by the cubic symmetry of the bcc lattice are more localized and reside in the neighborhood of −0.6 Ry and between −0.3 to −0.2 Ry, respectively. The complex bands of the solid clearly reflect the same band structure. However, the bands are slightly shifted and broadened because of the disorder scattering of Bloch states in the disordered alloy. The broadening due to disorder scattering are maximum for the Cu *d*-like bands, less for the Zn *d*-like bands, and minimum for the lower *s*-like bands. This is because Cu and Zn atoms do not present much fluctuation in the potential for the *s*-like states.

The same is reflected in the spectral functions, shown here also along the Γ-N direction in the Brillouin zone. Sharp peaks stretching from −0.8 Ry, groups of wider peaks around −0.6 Ry with less dispersion, are characteristic of the more localized *d*-like states and groups of much wider peaks straddling −0.3–0.2 Ry also with less dispersion. The spectral functions play an important role in response functions related to photoemission and optical conductivity.[56] Our complex bands agree remarkably well with Fig. 3 of Bansil and Ehrenreich.[4] These authors of course did not show the dispersion of the Zn *d* bands, but as in their work, the Cu bands show greater disorder-induced broadening than the lower-energy Zn *d* bands.

We may use the generalized tetrahedron method to pass from the reciprocal space spectral functions to the real space density of states.[57] Alternatively, we may also carry out real-space ASR to obtain the density of states directly.

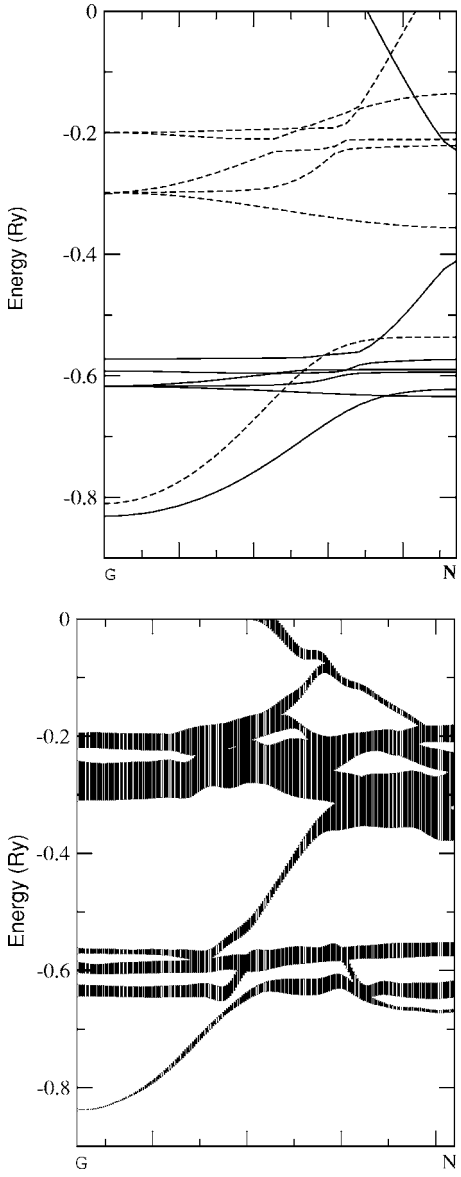

FIG. 1. (left) Bands for pure Cu and Zn in bcc lattices with the same lattice parameter as the 50-50 CuZn alloy. The dashed lines are for Cu and the full lines for Zn. (right) Complex bands for the 50-50 CuZn alloy.

Figure 3 shows the densities of states for the pure Zn (solid lines) and Cu (dashed lines) in the same bcc lattice as the alloy and compares this with the ordered B2 and disordered bcc 50-50 CuZn alloy. We first note that in the ordered B2 alloy there is a considerable narrowing of the Zn well as the Cu *d*-like bands. The feature around −0.35 Ry below the Fermi energy is suppressed in the ordered alloy. In the disordered alloy on the other hand, although disorder scattering introduces lifetime effects which washes out the sharp structures in the ordered systems, the resemblance to the pure metals is evident. As seen in the complex bands, the lifetime effects in the Cu *d*-like part is prominent. If we interpret the bottom-most Fig. 3(a) as that due to completely segregated CuZn and the middle one as the completely ordered one,

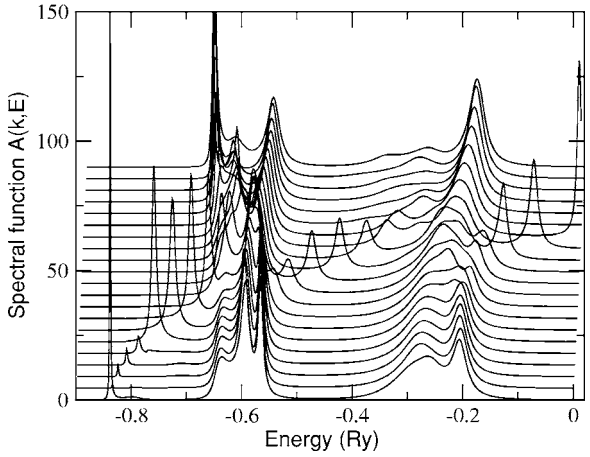

FIG. 2. Spectral functions for the CuZn alloy for **k** vectors along the Γ to *N* direction in the Brillouin zone.

then the disordered alloy lies between the two. In the next section, introducing short-range ordering effects on top of the fully disordered alloy, we shall study how to bridge between the two states.

III. SHORT-RANGED ORDERING IN THE ALLOYS

Attempts at developing generalizations of the coherent potential approximation (CPA) to include effects of short-range order (SRO) have been many, spread over the last several decades. The CPA being a single site mean-field approximation could not take into account SRO, since any de-

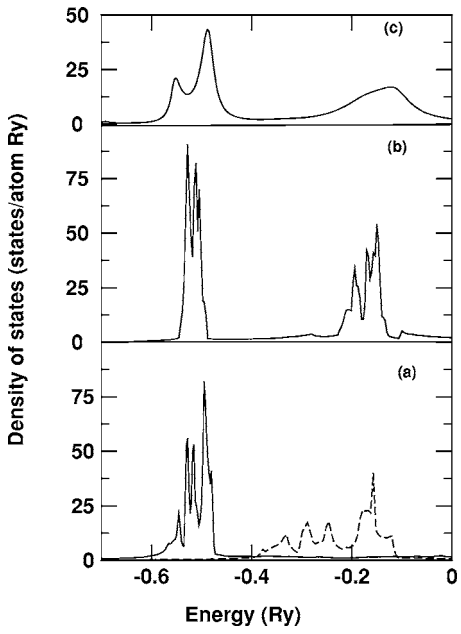

FIG. 3. (a) Density of states of pure Zn (solid lines) and Cu (dashed lines) in the same bcc lattice as the 50-50 CuZn alloy. (b) Density of states for ordered B2 50-50 CuZn alloy. (c) Density of states for the disordered bcc 50-50 CuZn alloy. These results are comparable to the single-site CPA.

scription of SRO had to take into account correlations in, at least, a nearest-neighbor cluster on the lattice. The early attempts to generalize the CPA to clusters were beset with difficulties of violation of the analytic properties of the approximated configuration averaged Green's function. Tsukada's[39] idea of introducing a supercell of the size of the cluster immersed in an effective medium suffered from the problem of broken translational symmetry within the cluster even when the disorder was homogeneous. The Cluster CPA proposed by Kumar *et al.*[40] based on the augmented space theorem also suffered from the same problem. The embedded cluster approximation of Gonis *et al.*[41] immersed a cluster in a CPA medium which lacked the full self-consistency with it. The first translationally symmetric cluster approximations which preserved the analytic properties of the approximate Green's functions were all based on the augmented space theorem of Mookerjee.[26] They included the traveling cluster approximation (TCA) of Kaplan and Gray[27,42] and Mills and Ratanavararaksa[43] and the Cluster CPA proposed by Razee *et al.*[44] The problem with these approaches was that they became intractable as the size of the cluster was increased much beyond two sites. Mookerjee and Prasad[45] generalized the augmented space theorem to include correlated disorder. However, since they then went on to apply it in the CCPA approximation, they could not go beyond the two-site cluster and they applied the method to model systems alone. The breakthrough came with the augmented space recursion (ASR) proposed by Saha *et al.*[46,47] The method was a departure from the mean-field approaches which always began by embedding a cluster in an effective medium which was then obtained self-consistently. Here the Green's function was expanded in a continued fraction whose asymptotic part was approximately estimated from its initial steps through an ingenious *termination* procedure.[33] In this method the effect at a site of quite a large environment around it could be taken into account depending how far one went down the continued fraction before *termination*. The technique was made fully LDA self-consistent within the tight-binding linear muffin-tin orbitals (TB-LMTO) approach[48] and several applications have been carried out to include short-range order in different alloy systems.[49] Recently Leath and co-workers have developed an itinerant CPA (ICPA) based on the augmented space theorem,[50] which also maintains both analyticity and translational symmetry and takes into account the effect of the nearest neighbor environment of a site in an alloy. The technique has been successfully applied to the phonon problem in alloys where there were large force constant disorders. The results of this method for NiPd and NiPt alloys match well with the ASR applied to the same alloys,[51] and there is now an effort to apply the ICPA to electronic problems based on both the TB-KKR and the TB-LMTO methods. A very different and rather striking approach has been developed by Rowlands *et al.*[52] (the nonlocal CPA or NL-CPA) using the idea of *coarse graining* in reciprocal space originally proposed by Jarrell and Krishnamurthy.[6] The NL-CPA with SRO has been applied earlier by Rowlands *et al.*[5] and is on the verge of being made fully DFT self-consistent within the KKR.[53] In this paper we report a fully DFT self-consistent ASR based on the TB-LMTO with SRO incorporated. We have applied it to the case of 50-50 CuZn alloys, so as to have a comparison with earlier attempts using different techniques.

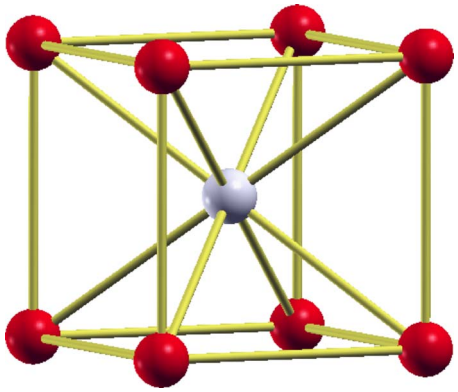

FIG. 4. (Color online) The light (blue) atom represents the site labeled 0, where the local density of states will be calculated. The dark (red) atoms are its eight nearest neighbors on the bcc lattice.

IV. THE GENERALIZED AUGMENTED SPACE THEOREM

The generalized augmented space theorem has been described in detail by Mookerjee and Prasad.[45] Let us briefly introduce those essential ideas which are necessary to make this communication reasonably self-contained.

For a substitutionally binary disordered alloy A_xB_y on a lattice we can introduce a set of random *occupation variables* $\{n_R\}$ associated with the lattice sites labeled by R, which take the values 0 or 1 depending upon whether the site R is occupied by a A or a B type of atom. The Hamiltonian and hence the Green's function are both functions of this set of random variables.

To start with, let us assume that short-range order extends up to nearest-neighbors only. Let us take for an example the nearest-neighbor cluster of nine atoms on a body-centered-cubic lattice (see Fig. 4) centered on the site (light colored in the figure) labeled by R_0. The occupation variables associated with its eight neighbors are correlated with n_{R_0}, but not with one another. Further none of the other occupation variables associated with more distant sites are correlated with n_{R_0}.

We may then write

$$P(n_{R_0}, n_{R_1}, \ldots n_{R_k} \ldots) = P(n_{R_0}) \prod_{j=1}^{8} P(n_{R_j}|n_{R_0}) \prod_{k>8} P(n_{R_k}).$$

The generalized augmented space theorem then associates with the random variables $\{n_{R_k}\}$ corresponding operators $\{\mathbf{M}_{R_k}\}$ in their configuration space. The construction of the representations of these operators has been discussed in detail in the paper by Mookerjee and Prasad.[45] Here we shall quote only the relevant results necessary to proceed further.

We shall characterize the SRO by a Warren-Cowley parameter α. In terms of this the probability densities are given by the following:

For $k=0$ and $k>8$,

$$P(n_{R_k}) = x\delta(n_{R_k}-1) + y\delta(n_{R_k}), \quad x+y=1.$$

For $1 \leq j \leq 8$,

$$P(n_{R_j}|n_{R_0}=1) = (x+\alpha y)\delta(n_{R_j}-1) + (1-\alpha)y\delta(n_{R_j}),$$

$$P(n_{R_j}|n_{R_0}=0) = (1-\alpha)x\delta(n_{R_j}-1) + (y+\alpha x)\delta(n_{R_j}).$$

In the full augmented space, the operators which replace the occupation variables are

$$\tilde{\mathbf{M}}_{R_0} = M_{R_0} \otimes I \otimes I \otimes \ldots,$$

$$\tilde{\mathbf{M}}_{R_j} = \sum_{\lambda=0}^{1} P_1^k \otimes M_{R_j}^{\lambda} \otimes I \otimes \ldots, \quad j=1,2,\ldots,8,$$

$$\tilde{\mathbf{M}}_k = I \otimes I \otimes \ldots M_{R_k} \otimes I \otimes \ldots, \quad k>8,$$

$$P(n_{R_j}|n_{R_0}=\lambda) = -\frac{1}{\pi}\lim_{\delta\to 0} \mathrm{Im}\langle\uparrow_{R_j}|[(n_{R_j}+i\delta) - M_{R_j}^{\lambda}]^{-1}|\uparrow_{R_j}\rangle. \tag{4}$$

We now follow the augmented space theorem and replace all the occupation variables $\{n_R\}$ by their corresponding operators. The configuration average is the specific matrix element between the *reference* state $|\{\varnothing\}\rangle$ as discussed earlier. We also note that the choice of the *central* site labeled R_0 is immaterial. If we translate this site to any other and apply the lattice translation to all the sites, the Hamiltonian in the full augmented space remains unchanged. This formulation of short-ranged order also possesses lattice translational symmetry, provided the short-range order is homogeneous in space.

V. EFFECT OF SRO ON THE DENSITY OF STATES

We have carried out the TB-LMTO-ASR calculations on CuZn with a lattice constant of 2.85 Å. The Cu and Zn potentials are obtained from the LDA self-consistency loop. All reciprocal space integrals are carried out by using the generalized tetrahedron integration for disordered systems introduced by us earlier.[57]

Let us discuss the effect of SRO, leading, on one hand to ordering ($\alpha<0$) and on the other to segregation ($\alpha>0$). We shall first look at Figs. 1 and 3. The complex band structure shown in Fig. 1 shows that the system is a *split band* alloy. The positions of the *d* bands of Cu and Zn are well separated in energy. This implies that the "electrons travel more easily between Cu or between Zn sites than between unlike ones."[5] So when the alloy orders and unlike sites sit next to each other, the overlap integral between the like sites decrease. This leads to a narrowing of the bands associated with Cu and Zn. A comparison between the bottom and central panels of Fig. 3 shows that the bands in the latter are much narrower than those of the former. This is the main effect of ordering setting in. On the other hand, when the alloy is completely disordered, the bands become widened by disorder scattering and the sharp structures in the density of states are smoothened.

Figure 5 (left panel) shows the density of states with increasing positive α indicating increasing clustering tendency. Comparing with Fig. 3 we note that as clustering tendency increases the density of states begins to show the structures seen in the pure metals in both the split bands. For large positive α there is still residual long-ranged disorder. This causes smoothening of the bands with respect to the pure materials. For these large, positive α's, we notice the development of the structure around −0.35 Ry below the Fermi energy.

Figure 5 (right panel) shows the density of states with increasing negative α indicating increasing ordering tendency. On the bcc lattice at 50-50 composition we expect this ordering to favor a B2 structure. With increasing ordering tendency, both the split bands narrow and lose structure. The feature around −0.35 Ry disappears. This band narrowing and suppression of the feature around −0.35 Ry is clearly seen in the ordered B2 alloy shown in Fig. 3(b).

Our analysis is closely similar to that of Rowlands *et al.*[5] Although there are differences in the way short-range order is introduced in the ASR and NL CPA, there is broad agreement between the two works on the effect of short-range ordering. In particular, the development of the shoulder around −0.35 Ry below the Fermi energy with segregation and the narrowing of the split bands on ordering are observed in both the approaches. In the ordering regime there are minor differences in the results of the two approaches. The relative heights of the two peaks in the split bands are much more pronounced and the broadening is larger in the ASR as compared with NL CPA.

Finally, in Fig. 6 we show the band energy as a function of the nearest-neighbor Warren-Cowley parameter. The minimum occurs at the ordering end, as expected. Experimentally, the alloy does show a tendency to order at lower temperatures.

VI. OPTICAL PROPERTIES OF CuZn ALLOYS

In an earlier work[54] we had developed a methodology for the calculation of configuration averaged optical conductivity of a disordered alloy based on the augmented space formalism. Here we shall present the main features of the method necessary to understand the calculation of optical response functions in the 50-50 CuZn alloy.

In linear response theory, at zero temperature, the generalized susceptibility of a disordered alloy is given by the Kubo formula

$$\chi^{\mu\nu}(t-t') = (i/\hbar)\Theta(t-t')\langle[\mathbf{j}^{\mu}(t)\mathbf{j}^{\nu}(t')]\rangle,$$

where $\mathbf{j}^{\mu}$ is the current operator and Θ is the Heaviside step function. If the underlying lattice has cubic symmetry, $\chi^{\mu\nu}=\chi\ \delta_{\mu\nu}$. The fluctuation-dissipation theorem then relates the imaginary part of the Laplace transform of the generalized susceptibility to the Laplace transform of a correlation function,

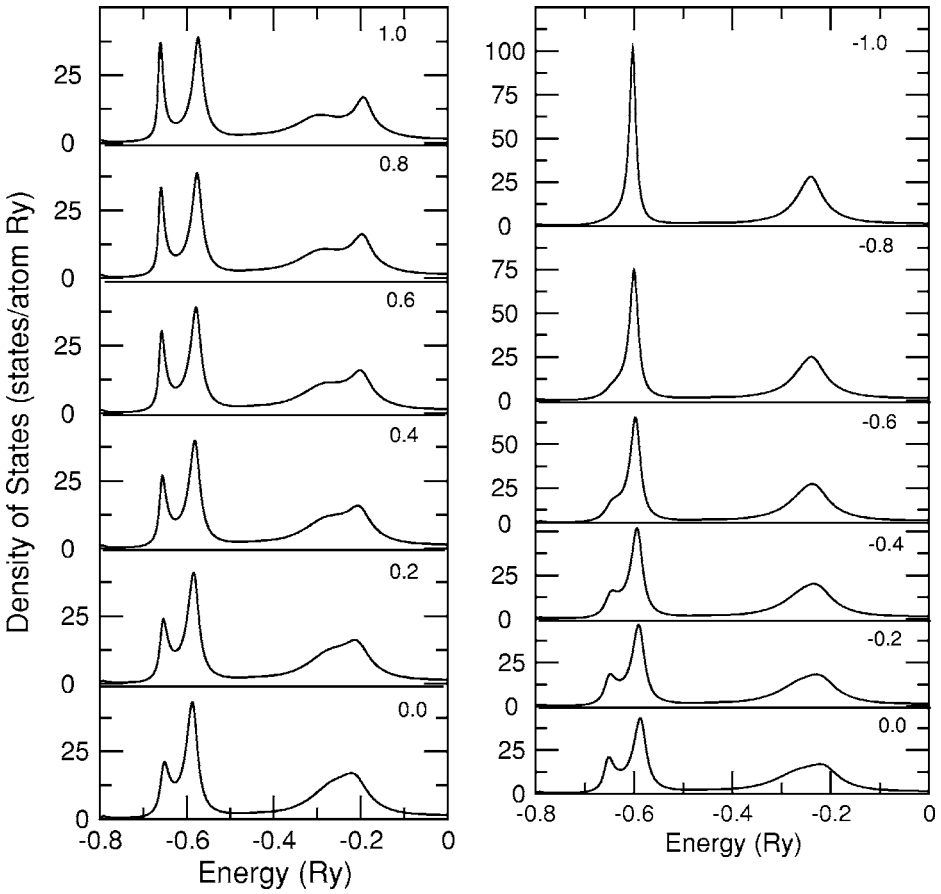

FIG. 5. Density of states for 50-50 CuZn with (left) increasing positive α which indicates increasing clustering tendency and (right) increasing negative α which indicates ordering tendency. The values of the SRO parameter α are shown on the upper right corner of each panel. Energies are shown with respect to the Fermi energy placed at the origin.

$$\chi''(\omega) = (1/2\hbar)(1 - \exp\{-\beta\hbar\omega\})S(\omega),$$

where

$$S(\omega) = \int_0^\infty dt \exp\{i(\omega + i\delta)t\}\mathrm{Tr}[\mathbf{j}^\mu(t)\mathbf{j}^\mu(0)]. \tag{5}$$

Since the response function is independent of the direction label μ for cubic symmetry, in the following we shall drop this symbol. In the case of other symmetries we have to generalize our results for different directions. Our goal will be, given a quantum "Hamiltonian" $\mathbf{H}^{(2)}$ to obtain the correlation function,

$$S(t) = \langle\phi|\mathbf{j}(t)\mathbf{j}(0)|\phi\rangle.$$

We shall now determine the correlation directly via the generalized recursion method as described by Viswanath and Müller.[55]

For a disordered binary alloy, $S(t) = S[\bar{\mathbf{H}}(\{n_R\})]$. The augmented space theorem then states that

$$\langle\langle S(t)\rangle\rangle = \langle\langle\langle\phi|\mathbf{j}(t)\mathbf{j}(0)|\phi\rangle\rangle\rangle = \langle\phi\otimes\{\varnothing\}|\tilde{\mathbf{j}}(t)\tilde{\mathbf{j}}(0)|\phi\otimes\{\varnothing\}\rangle$$
$$= S[\tilde{\mathbf{H}}(\{\tilde{\mathbf{M}}_R\})],$$

where the augmented space Hamiltonian and the current operators are constructed by replacing every random variable n_R by the corresponding operator $\tilde{\mathbf{M}}_R$. The recursion may now be carried out step by step in the full augmented space and the configuration averaged structure function, which is the Laplace transform of the averaged correlation function can then be obtained as a continued fraction,

$$\langle\langle S(\omega)\rangle\rangle = \lim_{\delta\to 0} 2\,\mathrm{Re}\,\tilde{d}_0(\omega + i\delta), \tag{6}$$

where

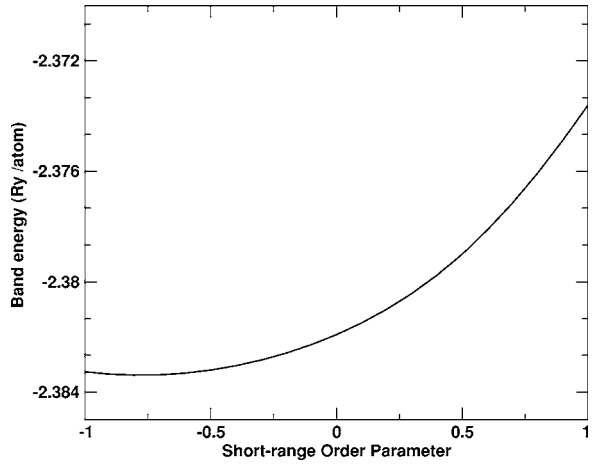

FIG. 6. The band energy (from which the contribution of the core electrons have been subtracted) as a function of the nearest-neighbor Warren-Cowley SRO parameter.

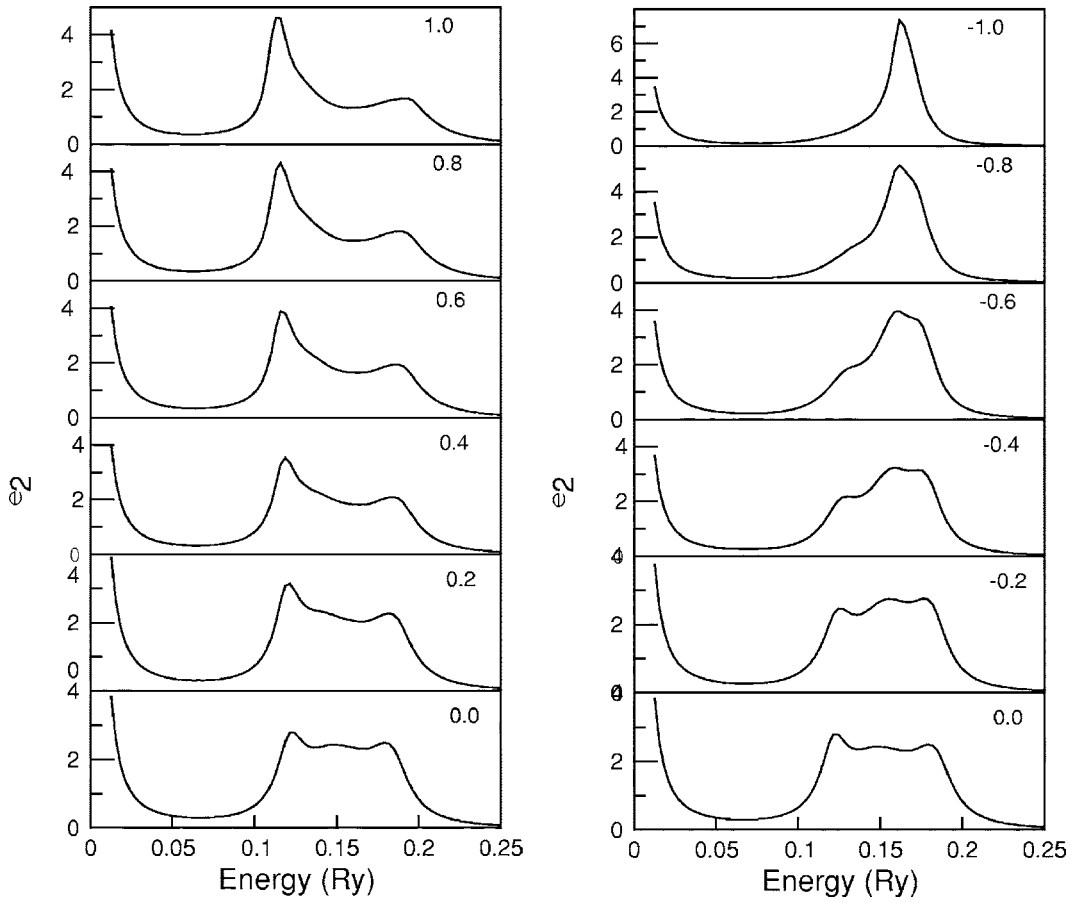

FIG. 7. (left panels) Imaginary part of the dielectric function as a function of energy and its variation with the nearest-neighbor Warren-Cowley SRO parameter, $\alpha > 0$ increasing, indicating segregating tendency. (right panels) The same with $\alpha < 0$ increasing, indicating ordering tendency. The value of α is given on the top right-hand corner of each panel.

$$\tilde{d}_0(z) = \cfrac{i}{z - \tilde{\alpha}_0 - \cfrac{\tilde{\beta}_1^2}{z - \tilde{\alpha}_1 - \cfrac{\tilde{\beta}_2^2}{z - \tilde{\alpha}_2 - \ldots}}}. \tag{7}$$

The imaginary part of the dielectric function is related to this correlation function through

$$\epsilon_2(\omega) = \frac{\langle\langle S(\omega)\rangle\rangle}{\omega}.$$

Equations (6) and (7) will form the basis of our calculation of the configuration averaged correlation function.

The real part of the dielectric function $\epsilon_1(\omega)$ is related to the imaginary part $\epsilon_2(\omega)$ by a Kramer's Krönig relationship. All optical response functions may now be derived from these. If we assume the orientation of the crystal surface to be parallel to the optic axis, the reflectivity $R(\omega)$ follows directly from Fresnel's formula

$$R(\omega) = \left| \frac{\sqrt{\epsilon(\omega)} - 1}{\sqrt{\epsilon(\omega)} + 1} \right|^2.$$

Figure 7 shows the imaginary part of the dielectric function varying with frequency. If we examine the density of states for both the ordered and disordered alloys we note that it is only around or just above $\hbar\omega \simeq 0.1$ Ry that the transitions from the d bands of Cu begin to contribute to $\epsilon_2(\omega)$. Below this energy, the behavior is Drude-like. This is clearly seen in the panels of the figure. As α increases and the alloy tends to segregate since the weight of the structure in the density of states nearer to the Fermi-energy increases, this contribution leads to the increasing weight of the structure near 0.1 Ry.

Figure 7 shows the variation of $\epsilon_2(\omega)$ with the nearest-neighbor Warren-Cowley SRO parameter. The narrowing of the band with ordering and the increase of weightage to the structure away from the Fermi energy is clearly reflected in the dielectric function. It is also obvious from the figures that the imaginary part of the dielectric function is more sensitive to the variation of short-range order than the density of states.

Color changes in CuZn brasses have been observed both with changing composition, hence different phase structures, and on heating.[19] In particular, as these alloys are colored, the changes can be observed visually. A study of the changes in optical reflectivity due to ordering or segregation would be interesting. The *color* of these alloys should be due to the same physical mechanism of internal photoelectric excitations, as proposed for colored metals such as Cu and Au. Of

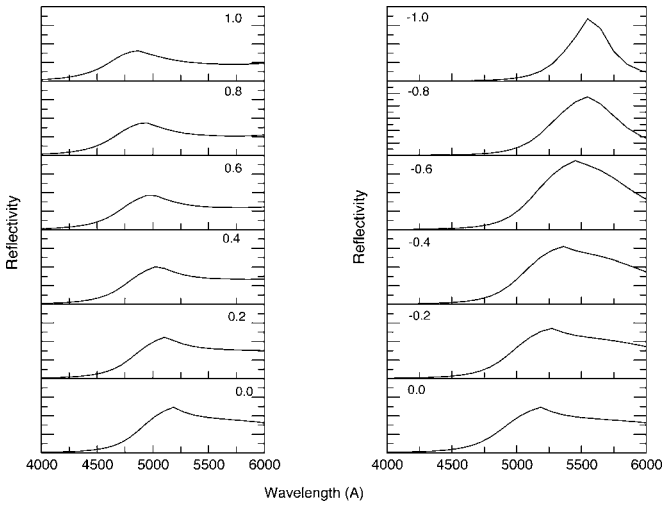

FIG. 8. (left panels) Reflectivity as a function of the wavelength and its variation with the nearest-neighbor Warren-Cowley parameter $\alpha>0$ increasing indicating segregating tendency. (right panels) The same with $\alpha < 0$ indicating ordering tendency. The values of α are given on the top corners of each panel.

course, we should take care of plasma effects and other phenomena that together and in a combined way give rise to *color*. However, it would be, as an initial study, examine the effect of SRO on the optical reflectivity of the alloy. This is shown in Fig. 8.

The first thing we note that for the completely disordered alloy the reflectivity has a maximum around $\lambda=5200$ Å which is not very different from that of Cu at low temperatures and is in the yellow-green region. Below this the reflectivity sharply drops (the reflectivity edge) and light of lower wavelengths is not reflected. With increasing segregation tendency this maximum drops almost linearly with α to around 4950 Å which is towards the green range. On the other hand with increasing ordering tendency the maximum moves out towards 5600 Å, that is, moves towards the yellow from the yellow-green wavelengths. We would expect then a shift from a yellow-green color in the disordered to a more yellow region in the ordered material. We should note that these calculations are all done at 0 K. In an actual experiment the disorder-order transition takes place with varying temperature and the temperature effects on the electronic structure must be taken into account, as well as effect of plasma oscillations. We shall leave this for a later paper.

VII. CONCLUSION AND COMMENTS

The work presented here is a part of our continuing development of methods for the study of electronic structure of disordered alloys based on the augmented space method introduced by one of us. We have argued that our generalization of the augmented space technique to include correlated disorder and its combination with the recursion method of Haydock[33] yields configuration averaged Green's functions which are lattice translationally symmetric and have the necessary Herglotz analytical properties of the exact ones. We have applied this technique to the case of the split-band alloy 50-50 CuZn. Experimental evidences of short-range ordering in this alloy exist and hence our interest in its study. We have looked at the whole range of short-range ordering from clustering to homogeneous disorder to ordering and have studied its effect on the density of states, optical conductivity, and reflectivity of the alloy. Our results are in broad agreement with an alternative approach via the nonlocal CPA.

We had set out to demonstrate that the generalized augmented space recursion, in combination with the LDA-based TB LMTO, is an efficient computational technique which can go beyond the single-site mean-field approximation and take into account local environmental effects like short-range ordering and clustering, at the same time maintaining analytic properties essential for physical interpretation of its results. This is the main conclusion of this work.

ACKNOWLEDGMENT

One of us (K.T.) would like to acknowledge the CSIR for financial assistance.

*Permanent address: Ramakrishna Mission Vivekananda Centenary College, Rahara, West Bengal, India.

[1] F. Jona and P. M. Marcus, J. Phys.: Condens. Matter **13**, 5507 (2001).
[2] *Binary Alloy Phase Diagrams*, edited by T. B. Massalski, H. Okamoto, P. R. Subramaniam, and L. Kacprzak (ASM International, Materials Park, OH 1990).
[3] W. Hume-Rotherý, *The Structure of Metals and Alloys* (Institute of Metals, London, 1936).
[4] A. Bansil and H. Ehrenreich, Phys. Rev. B **9**, 445 (1974).
[5] D. A. Rowlands, J. B. Staunton, B. L. Gyorffy, E. Bruno, and B. Ginatempo, Phys. Rev. B **72**, 045101 (2005).
[6] M. Jarrell and H. R. Krishnamurthy, Phys. Rev. B **63**, 125102 (2001).
[7] F. C. Nix and W. Shockley, Rev. Mod. Phys. **10**, 1 (1938).
[8] L. Guttman, in *Solid State Physics*, edited by F. Seitz and D. Turnbull (Academic Press, New York, 1956), Vol. 3.
[9] C. B. Walker and D. T. Keating, Phys. Rev. **130**, 1726 (1963).
[10] C. B. Walker and D. R. Chipman, Phys. Rev. B **4**, 3104 (1971).
[11] I. A. Abrikosov, A. M. N. Niklasson, S. I. Simak, B. Johansson, A. V. Ruban, and H. L. Skriver, Phys. Rev. Lett. **76**, 4203 (1996).
[12] I. A. Abrikosov, Yu. H. Velikov, P. A. Korzhavyi, A. V. Ruban, and L. E. Shilkrot, Solid State Commun. **83**, 867 (1992).
[13] D. D. Johnson and F. J. Pinski, Phys. Rev. B **48**, 11553 (1993).
[14] P. P. Singh, A. Gonis, and P. E. A. Turchi, Phys. Rev. Lett. **71**, 1605 (1993).
[15] P. P. Singh and A. Gonis, Phys. Rev. B **49**, 1642 (1994).
[16] P. A. Korzhavyi, A. V. Ruban, I. A. Abrikosov, and H. L. Skriver, Phys. Rev. B **51**, 5773 (1995).

[17] Y. Wang, G. M. Stocks, W. A. Shelton, D. M. C. Nicholson, Z. Szotek, and W. M. Temmerman, Phys. Rev. Lett. **75**, 2867 (1995).
[18] E. Bruno, L. Zingales, and A. Milici, Phys. Rev. B **66**, 245107 (2002).
[19] L. Muldawer, Phys. Rev. **127**, 1551 (1963).
[20] G. Joos and A. Klopfer, Z. Phys. **138**, 251 (1954).
[21] H. Amar and K. H. Johnson, Phys. Rev. **139**, A760 (1965).
[22] H. Amar, K. H. Johnson, and K. P. Wang, Phys. Rev. **148**, 672 (1966).
[23] H. Amar, K. H. Johnson, and C. B. Sommers, Phys. Rev. **153**, 655 (1967).
[24] T. Saha, I. Dasgupta, and A. Mookerjee, J. Phys.: Condens. Matter **6**, L245 (1994).
[25] A. Mookerjee, in *Electronic Structure of Clusters, Surfaces and Alloys*, edited by A. Mookerjee and D. D. Sarma (Taylor and Francis, London, 2001).
[26] A. Mookerjee, J. Phys. C **6**, 1340 (1973).
[27] T. Kaplan and L. J. Gray, Phys. Rev. B **15**, 3260 (1977).
[28] T. Saha, I. Dasgupta, and A. Mookerjee, J. Phys.: Condens. Matter **8**, 1979 (1996).
[29] S. Ghosh, N. Das, and A. Mookerjee, Int. J. Mod. Phys. B **21**, 723 (1999).
[30] I. Dasgupta, T. Saha, A. Mookerjee, and G. P. Das, J. Phys.: Condens. Matter **9**, 3529 (1997).
[31] O. K. Andersen, Phys. Rev. B **12**, 3060 (1975).
[32] O. K. Andersen and O. Jepsen, Phys. Rev. Lett. **53**, 2571 (1984).
[33] R. Haydock, *Solid State Physics* (Academic Press, New York, 1980), Vol. 35.
[34] N. Beer and D. G. Pettifor, in *The Electronic Structure of Complex Systems*, edited by P. Phariseau and W. M. Temmerman (Plenum, New York, 1982), pp. 769.
[35] R. Haydock, Philos. Mag. B **43**, 203 (1981); R. Haydock and R. L. Te, Phys. Rev. B **49**, 10845 (1994).
[36] R. Haydock, Ph.D thesis, University of Cambridge, United Kingdom, 1972.
[37] A. Chakrabarty and A. Mookerjee, Eur. Phys. J. B **44**, 21 (2005).
[38] A. V. Ruban and H. L. Skriver, Phys. Rev. B **66**, 024201 (2003).
[39] M. Tsukada, J. Phys. Soc. Jpn. **32**, 1475 (1972).
[40] V. Kumar, V. K. Srivastava, and A. Mookerjee, J. Phys. C **15**, 1939 (1982).
[41] A. Gonis, G. M. Stocks, W. H. Butler, and H. Winter, Phys. Rev. B **29**, 555 (1984).
[42] L. J. Kaplan and T. Gray, Phys. Rev. B **14**, 3462 (1976).
[43] R. Mills and P. Ratanavararaksa, Phys. Rev. B **18**, 5291 (1978).
[44] S. S. A. Razee, S. S. Rajput, R. Prasad, and A. Mookerjee, Phys. Rev. B **42**, 9391 (1990).
[45] A. Mookerjee and R. Prasad, Phys. Rev. B **48**, 17724 (1993).
[46] T. Saha, I. Dasgupta, and A. Mookerjee, Phys. Rev. B **50**, 13267 (1994).
[47] T. Saha, I. Dasgupta, and A. Mookerjee, J. Phys.: Condens. Matter **8**, 1979 (1996).
[48] A. Chakrabarti and A. Mookerjee, Eur. Phys. J. B **44**, 21 (2005).
[49] D. Paudyal, T. Saha-Dasgupta, and A. Mookerjee, J. Phys.: Condens. Matter **16**, 2317 (2004).
[50] S. Ghosh, P. L. Leath, and M. H. Cohen, Phys. Rev. B **66**, 214206 (2002).
[51] A. Alam and A. Mookerjee, Phys. Rev. B **69**, 024205 (2004).
[52] D. A. Rowlands, J. B. Staunton, and B. L. Györffy, Phys. Rev. B **67**, 115109 (2003).
[53] D. A. Rowlands, J. B. Staunton, B. L. Györffy, E. Bruno, and B. Ginatempo, Phys. Rev. B **72**, 045101 (2005).
[54] K. Tarafder and A. Mookerjee, J. Phys.: Condens. Matter **17**, 6435 (2005).
[55] V. S. Viswanath and G. Müller, *The User Friendly Recursion Method* (Troisieme Cycle de la Physique, Suisse Romande, 1993).
[56] K. K. Saha and A. Mookerjee, J. Phys.: Condens. Matter **17**, 4559 (2005).
[57] K. K. Saha, A. Mookerjee, and O. Jepsen, Phys. Rev. B **71**, 094207 (2005).